Evaluation of Multirate Loss Models for the X2 Link of LTE Networks

P. I. Panagoulias and I. D. Moscholios

Dept. of Informatics & Telecommunications, University of Peloponnese, 221 00 Tripolis, Greece
E-mails: panagoulias@uop.gr, idm@uop.gr

***Abstract*–In this paper we review two multirate loss models, whereby we can assess the call-level QoS of the Long Term Evolution (LTE) X2 link supporting calls of different service-classes with fixed bandwidth requirements. The X2 interface connects directly two neighboring evolved NodeBs and is mainly responsible for the transfer of user-plane and control-plane data during a handover. In the first model, the impact of user mobility in congestion probabilities is studied. In the second model, a fluid mobility model is considered for the determination of congestion probabilities. In both models, the X2 interface is modeled as a link of fixed capacity. Handover calls are accepted in the X2 link whenever there exists available bandwidth. Otherwise, calls are blocked and lost. For the evaluation of both models we compare the QoS index of congestion probabilities, under the same offered traffic-load conditions. Analytical congestion probabilities results show that both models perform equally well in most cases.**

I. Introduction

Long Term Evolution (LTE) networks provide increased throughputs via better spectrum exploitation and the use of multiple antennas, minimized latencies and a relatively simplified (the so-called "flat") architecture for the Evolved UMTS Terrestrial Radio Access Network (E-UTRAN) [1]. LTE market penetration is mainly attributed to the fact that the LTE technology is based on the 3G UMTS technology, meaning that no extensive network equipment upgrade and modifications are required, making the 3G to 4G migration for network operators easier and less costly.

The main components of an LTE network are the Evolved Packet Core (EPC) and the E-UTRAN. The EPC is responsible for the management of the core network components and the communication with the external network. The E-UTRAN provides air interface, via evolved NodeBs (eNBs), to a User Equipment (UE) and acts as an intermediate node handling the radio communication between the UE and the EPC. Each eNB covers a specific cell and exchanges traffic with the core network through the S1 interface. An active UE is quite likely to cross the boundary of the source cell, causing a handover. A handover is the process of a seamless transition of the UE's radio link from the source eNB to one of its neighbors. During this transition, the direct logical interface (link) between two neighboring eNBs – the X2 link – is used, for the user data arriving to the source eNB via the S1 link, to be transferred to the target eNB (Fig. 1).

The X2 interface is mainly used for the handover operation but it also supports load management and inter-cell interference coordination functions. However, considering that load management requires a constant but negligible bandwidth and assuming homogeneous LTE networks (all eNBs have similar characteristics and serve roughly the same number of users), in which interference coordination is not used (see e.g, [2], [3]), we consider only the bandwidth required for the handover support.

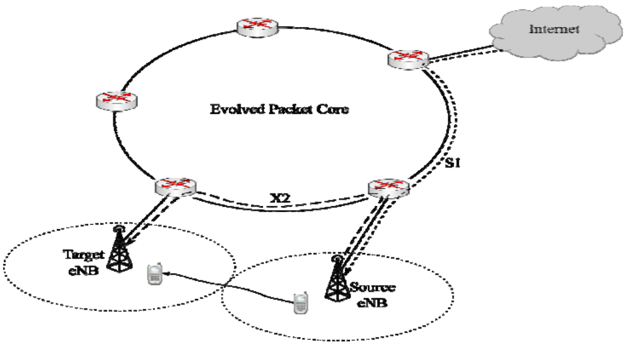

Figure 1. The S1 interface and the X2 interface between source and target eNBs.

Based on the above, the X2 link carries both control and user plane traffic. However, according to [4]-[5], control plane traffic can be considered negligible compared to user plane traffic. Therefore, we take into account user plane traffic. In addition, due to the assumption of a homogeneous LTE network, the outgoing user plane traffic, originated by UEs leaving a cell, is equal to the incoming user plane traffic, originated by UEs entering a cell [4]. Therefore, we consider only outgoing user plane traffic and focus on the calculation of congestion probabilities in the X2 link.

A literature review shows that the determination of congestion probabilities in the X2 link can be based on multirate teletraffic loss models (see e.g., [2], [4]-[5]). In [2], a simple model is proposed that studies the impact of UE mobility in congestion probabilities. A circular source cell is considered, that accommodates a finite number of users, who generate quasi-random handover traffic [6] and have different bandwidth requirements. All UEs are considered having a constant velocity and moving in a straight line. The X2 link is modeled as a link of fixed capacity that accepts handover calls if their total bandwidth requirement is available upon their arrival. The calculation of congestion probabilities is based on analytical formulas that take into account UEs mobility, but can be complex in the case of large systems with large capacities and many service-classes. This is because enumeration and processing of the state space is required. In [4], a richer stochastic model is proposed, which is based on a fluid mobility model (e.g., [7]-[8]) and the classical Erlang Multirate Loss Model (EMLM) [9]-[10]. Calls arrive in the X2 link according to a Poisson process and compete for the available bandwidth under the Complete Sharing (CS policy). In the CS policy, a call is accepted in the system if its bandwidth requirement is available. Otherwise, the call is blocked and lost without further affecting the system. Although the models of [2] and [4] provide similar congestion probability results in most cases (see Section IV), the model of [4] is preferable since: a) basic performance measures including congestion probabilities, link utilization and average number of calls in the system can be recursively determined, without the need of state space processing, b) it can be extended to evaluate the call-level QoS of the X2 link under various other bandwidth sharing policies (e.g., the bandwidth reservation policy [11]-[13] or the threshold policy [14]-[16]) and c) different handover arrival processes can be studied, e.g., the batched Poisson process or an ON-OFF process [17]-[20]. Finally, in [5], a multirate loss model is proposed, based on the EMLM, assuming that traffic in the X2 link is elastic. Elastic traffic refers to calls whose bandwidth is not fixed during their lifetime in the system. For a recent paper that also considers elastic traffic in LTE access networks but focuses on flow/packet level (not on call-level as [2], [4]-[5]) and determines transfer delay based on simple queueing models (the M/G/R-Processor Sharing and the M/D/1 models), the interested reader may resort to [21].

In this paper, we review [2], [4] and study the pros and cons of each model. Numerical results on congestion probabilities show that both models perform equally well, under the same offered traffic-load conditions, especially when a modified version of [2] is considered (see Section IV).

This paper is organized as follows: In Section II, we review the model of [2], proposed by Blogowski, Klopfenstein and Renard (BKR model). In Section II.A, we consider the single-service case while in Section II.B, we consider the multi-service case. In Section III, we review the model of [4], proposed by Widjaja and La Roche (WLR model). In Section IV, we present the relationship between both models. In Section V, we present analytical congestion probabilities results for both models and show the cases where both models provide similar congestion probabilities results. We conclude in Section VI.

II. The BKR Model

A. The single-service case

Consider a circular source cell of radius R (in m) which accommodates a single UE. The UE is considered having a constant velocity v (in m/s), moving in a straight line and communicating for a constant duration of Δ (in s). During the time Δ, the UE covers a distance of $v\Delta$. If $v\Delta \geq 2R$, then the UE leaves the source cell with probability $P_{exit} = 1$ and moves to the target cell (of the same radius R). On the other hand, if $v\Delta < 2R$, then the UE may leave the cell with probability P_{exit} or remain in the cell with probability $P_{stay} = 1 - P_{exit}$ depending on the UE's starting position in the source cell. Assuming that the starting position of the UE is uniformly distributed and since the circle is invariant under rotation, then P_{stay} is calculated by the ratio of the grey area S (area of two overlapping cells) of Fig. 2 and the area of a circle [2]:

$$P_{stay} = \frac{area(S)}{\pi R^2} \tag{1}$$

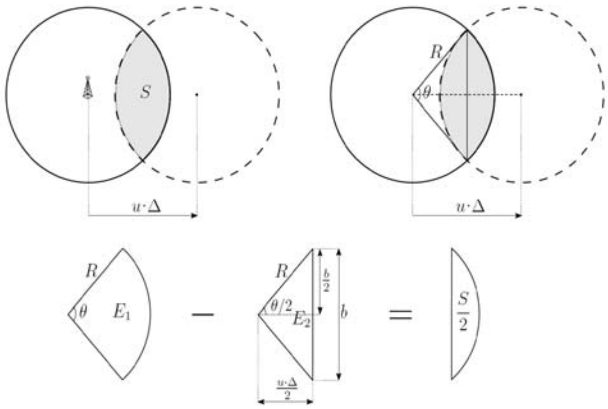

Figure 2. The grey area *S* defines the probability that the UE remains in the source cell. To determine *S*, subtract the area *E*2 from the area *E*1 of the circular sector, and multiply the result by 2, i.e., *S* = 2(*E*1-*E*2).

Based on (1) and assuming that $v\Delta < 2R$, P_{exit} can be determined by [2]:

$$P_{exit} = 1 - \frac{1}{\pi}\left(2\arccos\left(\frac{v\Delta}{2R}\right) - \frac{v\Delta}{R}\sqrt{1-\left(\frac{v\Delta}{2R}\right)^2}\right) \tag{2}$$

or according to Maclaurin series expansion:

$$P_{exit} \approx 2v\Delta / \pi R \tag{3}$$

for small values of $v\Delta/2R$.

The probability that a UE leaves the source cell at a given slot s of duration δ ms can be calculated by [2]:

$$P_{exit}(s) = \frac{\delta}{\Delta} P_{exit} \tag{4}$$

or based on the approximate formula of (3) by:

$$P_{exit}(s) = 2v\delta / \pi R \tag{5}$$

where it is assumed that the duration Δ is discretized in Δ/δ segments of size δ. Note that (5) is quite accurate, as δ is a very small quantity (in the order of ms) and consequently $P_{exit}(s)$ has a near-zero value (condition for the convergence to (2)).

Equation (3) has the following characteristics:

a) It expresses the average number of handovers during a communication. It is not only intuitively expected, since a UE will not do more than one handover during its communication, but it has also been proved in [22] (replace (16) in (36) of [22] to obtain (3) of our paper). According to [22], an underlying assumption for the proof of (3) is that the probability that a handover fails is zero (see Method II, pp. 1248 of [22]).

b) If $P_{exit} = 1$, then the maximum time a UE spends in the cell is $\Delta_{\max} \approx \pi R/2v$. The same result has been proved in [23] (see (5), pp. 604) for the mean sojourn time of a UE in an arbitrary cell, assuming that the UE enters the cell in a point A and leaves the cell in a point B (see Fig. 3). Two basic assumptions for the proof of [23] are: 1) the UE's velocity remains the same in the source and target cells and 2) the values of θ in Fig. 3 are given by $-\pi/2 < \theta < \pi/2$.

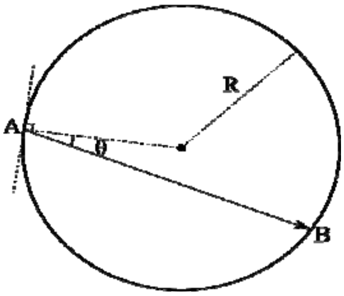

Figure 3. Sojourn time in an arbitrary cell [23].

The movement of the UE from the source eNB to the target eNB (with probability P_{exit}) causes the interruption of the radio link between the source eNB and the UE for δ ms (in the order of 25 to 50 ms). During this time δ, the source eNB is responsible for transferring to the target eNB, via the X2 link, an amount Q of data (in Mb). The latter consists of data already buffered at the source eNB and data that continue to arrive at the source eNB via the S1 link. Therefore, the capacity C_{X2} (in Mb/s) required for this data transfer of only one UE is given by [2]:

$$C_{X2} = Q/\delta \tag{6}$$

If we further denote by d (in Mb/s) the UE's data rate on the S1 link, then [2]:

$$Q = \beta d \tag{7}$$

where β is the period of time during which data are stored in the buffer (in the order of 100 ms).
Equation (6) due to (7), takes the form:

$$C_{X2} = \beta d/\delta \tag{8}$$

Consider now the case of N active UEs in the source cell and assume that all UEs have the same traffic and mobility characteristics. Then, the probability that there are exactly r UEs (out of N) leaving the cell simultaneously at a slot s of duration δ ms, $P_{ex}(r, N)$, is given by [2]:

$$P_{ex}(r,N) = \binom{N}{r}\left(P_{exit}\frac{\delta}{\Delta}\right)^{r}\left(1-P_{exit}\frac{\delta}{\Delta}\right)^{N-r} \tag{9}$$

while the probability that r or more UEs leave simultaneously the cell at a slot s is given by:

$$P_{ex}(x \ge r,N) = \sum_{x=r}^{N} P_{ex}(x,N) = \sum_{x=r}^{N}\binom{N}{x}\left(P_{exit}\frac{\delta}{\Delta}\right)^{x}\left(1-P_{exit}\frac{\delta}{\Delta}\right)^{N-x} \tag{10}$$

If exactly r UEs leave the source cell at a slot s then an amount rQ of data should be transferred via the X2 link. Therefore, the required capacity $C_{X2,r}$ for r UEs is [2]:

$$C_{X2,r} = rQ/\delta = r\beta d/\delta \tag{11}$$

while the probability, $P_{C_{X2,r}}(r)$, that the X2 link requires a capacity up to $r\beta d / \delta$ is:

$$P_{C_{X2,r}}(r) = \sum_{i=0}^{r} P_{ex}(i,N) = \sum_{i=0}^{r}\binom{N}{i}\left(P_{exit}\frac{\delta}{\Delta}\right)^{i}\left(1-P_{exit}\frac{\delta}{\Delta}\right)^{N-i} \tag{12}$$

As far as a UE's congestion probability is concerned, named herein Call Congestion (CC) probability, $P_{CC}(r)$, it expresses the case whereby a UE leaves the source cell on the same time slot as r or more other UEs and can be calculated by [2]:

$$P_{CC}(r) = \sum_{s=1}^{\Delta/\delta} P_{exit}(s) P_{ex}(x \ge r, N-1) \tag{13}$$

where we have excluded the reference UE from the N UEs, in order to calculate its CC probability.

Based on (4) and (10), (13) takes the form:

$$P_{CC}(r) = P_{exit}\sum_{x=r}^{N-1} P_{ex}(x, N-1) \tag{14}$$

B. The multi-service case

Consider now the case of K different service-classes accommodated in the source cell. We assume that the capacity of the X2 link is fixed and equal to C_{X2}. Let N_k be the number of active UEs of service-class, $k = 1,\ldots,K$ and $\boldsymbol{N} = (N_1,\ldots,N_k,\ldots,N_K)$ the corresponding vector. A service-class k active UE has a data rate d_k, a constant velocity v_k, a communication duration Δ_k, a probability $P_{exit,k}$ (given by (3)) and an amount of data Q_k that should be transferred via the X2 link in case of handover. Let also $r_k \le N_k$ be the number of service-class k UEs that leave the cell at a slot s of duration δ ms and $\boldsymbol{r} = (r_1,\ldots,r_k,\ldots,r_K)$ the corresponding vector.

Then, the probability $P_{ex}(\boldsymbol{r},\boldsymbol{N})$ is expressed by [2]:

$$P_{ex}(\boldsymbol{r},\boldsymbol{N}) = \prod_{k=1}^{K} P_{ex,k}(r_k, N_k) \tag{15}$$

where:

$$P_{ex,k}(r_k,N_k) = \binom{N_k}{r_k}\left(P_{exit,k}\frac{\delta}{\Delta_k}\right)^{r_k}\left(1-P_{exit,k}\frac{\delta}{\Delta_k}\right)^{N_k-r_k} \tag{16}$$

The CC probability of an active service-class k UE is determined by:

$$P_{CC,k}(\boldsymbol{r}) = P_{exit,k}\sum_{\boldsymbol{l}\in T_k} P(\boldsymbol{l}, \boldsymbol{N}_k^{-}) \tag{17}$$

where:

$\boldsymbol{N}_k^- = (N_1,...,N_k - 1,...,N_K)$,

$T_k = \left\{ \boldsymbol{l} \in \boldsymbol{H}_{\boldsymbol{N}_k^-} \left| \sum_{i=1}^{K} \frac{r_i \beta_i d_i}{\delta} + \frac{\beta_k d_k}{\delta} > C_{X2} \right. \right\}$ and

$\boldsymbol{H}_{\boldsymbol{N}} = \left\{ \boldsymbol{r} \left| r_k \leq N_k \right. \right\}$,

$\boldsymbol{H}_{\boldsymbol{N}_k^-} = \left\{ \boldsymbol{r} \left| r_i \leq N_i \; for \; i = 1,...,K \; and \; i \neq k, r_k \leq N_k - 1 \right. \right\}$.

Equation (17) shows a drawback of the BKR model: the determination of CC probabilities requires enumeration and processing in order to obtain the state space T_k. This procedure is quite complex especially for large capacity systems that accommodate many service-classes. On the other hand, the WLR model of Section III circumvents this problem by proposing an accurate and recursive formula for the calculation of CC probabilities.

III. The WLR Model

Consider a circular source cell of radius R which accommodates Poisson arriving calls of K different service-classes. Calls of service-class k (k=1,…,K) follow a Poisson process with arrival rate λ_k and have a generally distributed service time, μ_k^{-1}. Contrary to the BKR model, in the WLR model a fluid mobility model is considered for the determination of the offered traffic-load in the X2 link.

The fluid mobility model of [4] considers traffic flow as the flow of a fluid. Such a model can be used to model the behavior of macroscopic movement (i.e., the movement of an individual UE is considered of little significance) [8]. This fluid mobility model formulates the amount of traffic flowing out of a circular region of a source cell to be proportional to the population density within that region, the average velocity, and the length of the region boundary. For a circular region with a population density of ρ_k (UEs of service-class k per km^2), an average velocity of v_k, and a perimeter of L=2πR, the UE crossing rate per unit time, CR_k, from a source to any neighbor cell is:

$$CR_k = \rho_k v_k L / \pi = 2 \rho_k v_k R \tag{18}$$

Equation (18) is actually Thomas' formula [24] and can be used for various UE's mobility models (see e.g., [25]). Note that two limitations of fluid mobility models are the following: 1) they cannot be applied to cases where individual movement patterns are desired and 2) they are more accurate for regions of a large UE population [26].

Based on the above and assuming Poisson handover traffic, the offered traffic-load of service-class k calls, a_k, in the X2 link equals [4]:

$$a_k = p_A(k) \frac{\rho_k v_k L}{\pi} \delta = 2 p_A(k) \rho_k v_k R \delta \tag{19}$$

where: $p_A(k) = \lambda_k / (\lambda_k + \mu_k)$ is the probability that a service-class k UE is active (i.e., when there exists a Radio Resource Control (RRC) connection between a UE and eNB) and δ is the interruption time of the radio link between the source eNB and the UE, as defined in Section II.

Let b_k be the data rate of an active service-class k UE and n_k be the in-service service-class k UEs in the X2 link. By defining the corresponding vectors $\boldsymbol{n} = (n_1,...,n_k,...,n_K)$ and $\boldsymbol{b} = (b_1,...,b_k,...,b_K)$ then the occupied bandwidth j in the X2 link can be expressed as:

$$j = \boldsymbol{nb} = \sum_{k=1}^{K} n_k b_k, \;\; j = 0,1,...,C_{X2} \tag{20}$$

To determine the X2 link occupancy distribution, $q(j)$, it is assumed that UEs compete for the available bandwidth under the CS policy. Following the analysis of the classical EMLM, the un-normalized values of $q(j)$'s can be accurately determined by the classical Kaufman-Roberts recursive formula:

$$q(j) = \left\langle \begin{array}{c} 1 \; for \; j = 0 \\ \frac{1}{j} \sum_{k=1}^{K} a_k b_k q(j - b_k) \; for \; j = 1,...,C_{X2} \\ 0 \; otherwise \end{array} \right\rangle \tag{21}$$

Having determined $q(j)$'s we calculate the Time Congestion (TC) probabilities of service-class k, B_k, by the formula [4]:

$$B_k = \sum_{j=C_{X2}-b_k+1}^{C_{X2}} G^{-1} q(j) \tag{22}$$

where: $G = \sum_{j=0}^{C_{X2}} q(j)$ is the normalization constant.

TC probabilities are determined by the proportion of time the system is congested and can be measured by an outside observer. CC probabilities refer to the probability that a UE is blocked and lost. Due to the assumption of Poisson arrivals, TC and CC probabilities coincide (PASTA property, [6]).

IV. Relationship Between The Two Models

Based on Section II.B, the total offered traffic-load of service-class k UEs in the X2 link, $a_k^{'}$, of the BKR model is given by:

$$a_k^{'} = N_k P_{exit,k} \frac{\delta}{\Delta_k} = 2 \frac{N_k v_k \delta}{\pi R} \tag{23}$$

where: $P_{exit,k} = 2 v_k \Delta_k / \pi R$ while the term $2 v_k \delta / \pi R$ refers to the offered traffic-load of a single UE of service-class k in the X2 link.

Equation (23) coincides with (19) (of the WLR model) if we replace in (19) the population density $\rho_k = N_k / \pi R^2$ for a circular region and assume that UEs are always active.

According to [2], if we use (19) in (21) then the CC probabilities of the WKR model (obtained by (22)) are quite close to the corresponding probabilities of the BKR model (obtained by (17)) if we multiply B_k of (22) by $P_{exit,k} = 2 v_k \Delta_k / \pi R$. Although this is true in many examples, in Section V we show that there are cases where the CC probabilities results are not quite close. This is true especially for the CC probabilities of service-classes with low data rates requirements compared to C_{X2}

or to the bandwidth requirements of the other service-classes. To solve this problem, we follow the rationale of (22) and modify in (17) the state space T_k to the new:

$$T_k^{'} = \left\{ \boldsymbol{l} \in \boldsymbol{H}_{\boldsymbol{N}_k^-} \left| C_{X2} - \beta_k d_k + 1 \le \sum_{i=1}^{K} r_i \beta_i d_i + \beta_k d_k \le C_{X2} \right. \right\}.$$

We name this case, modified BKR model. Note that the new state-space $T_k^{'}$ comprises less congestion states compared to T_k, a fact that leads to the convergence of CC probabilities (between the two models) for service-classes with low data rates requirements.

V. Numerical Examples - Evaluation

In this section, we present three application examples and provide analytical CC probabilities results of the BKR model and its modified version as well as the WLR model.

In the first example, presented in [2], we consider three service-classes (VoIP, video, data) accommodated in a X2 link of capacity C_{X2} = 5120 Kbps. The data rates of VoIP, video and data are: d_1 = 32 kbps, d_2 = 320 kbps and d_3 = 1024 kbps, respectively. The other input parameters are the following: R = 250 m, $v_1 = v_2 = v_3$ = 12 km/h, δ = 25 ms, $\beta_1 = \beta_2 = \beta_3$ =100 ms, Δ_1 = 100 s, Δ_2 = 200 s (truncated to $\Delta_{max} = \pi R/2v_3$ = 117.81 s) and Δ_3 = 5 s. For the WLR model, we have $b_k = \beta_k d_k / \delta$ for k = 1, 2, 3.

Table 1a presents the CC probabilities obtained by the BKR model and the WLR model, while Table 1b presents the corresponding results for the modified BKR model. In the 1st column of Tables 1a, 1b we present the total number N of active UEs accommodated in the source cell. Based on the value of N and a distribution of 25%, 25% and 50% for each service-class, we obtain the corresponding values N_1, N_2 and N_3 for VoIP, video and data. As an example, when N = 20 active UEs, then N_1 = 5, N_2 = 5 and N_3 = 10. Similarly, when N = 200 active UEs, then N_1 = 50, N_2 = 50 and N_3 = 100. According to the results of Tables 1a, 1b we conclude that: 1) an increase in N results in the CC probabilities increase 2) the CC probabilities of the BKR and WLR model diverge when the data rate requirement of a service class (VoIP) is small compared to C_{X2} and 3) the CC probabilities of the modified BKR model are quite close to the corresponding results of the WLR model.

In the second example, we double the velocity (from 12 to 24 km/h), letting intact all other parameters. Note that now, both call durations Δ_1 and Δ_2 must be truncated to the maximum allowed value of 58.90 s.

Tables 2a and 2b present the corresponding CC probabilities results. We observe that the increase of velocity increases the respective (compared to the first example) CC probabilities of all service classes. Considering that the increase of velocity reduces the time a user spends in the source cell (and increases P_{exit}), this result was anticipated. Expanding this rationale we can find similar correlations between the other parameters and the CC probabilities. The results of the modified BKR model and the WLR model remain close as well.

In the third example, we keep the input of the second example and increase the interruption time δ from 25 to 50 ms. This causes a reduction (by a factor of 2) of the bandwidth that should be reserved in X2 link for each handover and consequently the respective (compared to the second example) CC probabilities are also reduced (see Tables 3a and 3b). The other conclusions drawn previously are valid in this example as well.

Table 1a: CC probabilities – 1st example (BKR, WLR)

	BKR			WLR		
N	$P_{cc,1}$	$P_{cc,2}$	$P_{cc,3}$	B_1	B_2	B_3
20	3.62E-06	2.12E-03	1.26E-04	4.42E-14	2.12E-03	1.35E-04
40	1.49E-05	4.24E-03	2.60E-04	7.11E-13	4.22E-03	2.69E-04
60	3.36E-05	6.35E-03	3.94E-04	3.59E-12	6.31E-03	4.02E-04
80	5.99E-05	8.45E-03	5.28E-04	1.13E-11	8.38E-03	5.34E-04
100	9.37E-05	1.06E-02	6.61E-04	2.74E-11	1.04E-02	6.65E-04
120	1.35E-04	1.27E-02	7.94E-04	5.66E-11	1.25E-02	7.96E-04
140	1.83E-04	1.47E-02	9.26E-04	1.04E-10	1.45E-02	9.26E-04
160	2.39E-04	1.68E-02	1.06E-03	1.78E-10	1.66E-02	1.06E-03
180	3.02E-04	1.89E-02	1.19E-03	2.83E-10	1.86E-02	1.18E-03
200	3.73E-04	2.10E-02	1.32E-03	4.30E-10	2.06E-02	1.31E-03

Table 1b: CC probabilities – 1st example (modified BKR)

	Modified BKR		
N	$P_{cc,1}$	$P_{cc,2}$	$P_{cc,3}$
20	8.58E-15	2.12E-03	1.26E-04
40	3.59E-13	4.22E-03	2.60E-04
60	2.32E-12	6.31E-03	3.93E-04
80	8.21E-12	8.38E-03	5.25E-04
100	2.13E-11	1.04E-02	6.57E-04
120	4.60E-11	1.25E-02	7.88E-04
140	8.76E-11	1.45E-02	9.18E-04
160	1.52E-10	1.66E-02	1.05E-03
180	2.47E-10	1.86E-02	1.18E-03
200	3.80E-10	2.06E-02	1.30E-03

Table 2a: CC probabilities – 2nd example (BKR, WLR)

	BKR			WLR		
N	$P_{cc,1}$	$P_{cc,2}$	$P_{cc,3}$	B_1	B_2	B_3
20	1.71E-05	4.24E-03	5.03E-04	8.38E-13	4.22E-03	5.37E-04
40	6.97E-05	8.45E-03	1.04E-03	1.33E-11	8.38E-03	1.07E-03
60	1.58E-04	1.27E-02	1.57E-03	6.67E-11	1.25E-02	1.59E-03
80	2.80E-04	1.68E-02	2.10E-03	2.09E-10	1.66E-02	2.11E-03
100	4.37E-04	2.10E-02	2.62E-03	5.06E-10	2.06E-02	2.62E-03
120	6.28E-04	2.51E-02	3.15E-03	1.04E-09	2.45E-02	3.13E-03
140	8.52E-04	2.93E-02	3.67E-03	1.91E-09	2.84E-02	3.63E-03
160	1.11E-03	3.34E-02	4.18E-03	3.24E-09	3.23E-02	4.12E-03
180	1.40E-03	3.75E-02	4.69E-03	5.14E-09	3.61E-02	4.61E-03
200	1.72E-03	4.16E-02	5.20E-03	7.78E-09	3.99E-02	5.10E-03

Table 2b: CC probabilities – 2nd example (modified BKR)

	Modified BKR		
N	$P_{cc,1}$	$P_{cc,2}$	$P_{cc,3}$
20	1.61E-13	4.22E-03	5.02E-04
40	6.71E-12	8.39E-03	1.03E-03
60	4.33E-11	1.25E-02	1.56E-03
80	1.52E-10	1.66E-02	2.08E-03
100	3.94E-10	2.06E-02	2.59E-03
120	8.47E-10	2.45E-02	3.10E-03
140	1.60E-09	2.84E-02	3.60E-03
160	2.78E-09	3.23E-02	4.09E-03
180	4.49E-09	3.61E-02	4.58E-03
200	6.88E-09	3.99E-02	5.06E-03

Table 3a: CC probabilities – 3rd example (BKR, WLR)

	BKR			WLR		
N	$P_{cc,1}$	$P_{cc,2}$	$P_{cc,3}$	B_1	B_2	B_3
20	7.33E-08	1.82E-07	2.20E-06	3.79E-24	1.51E-07	3.04E-06
40	6.94E-07	1.72E-06	1.04E-05	1.26E-21	1.19E-06	1.21E-05
60	2.46E-06	6.06E-06	2.46E-05	3.95E-20	3.97E-06	2.70E-05
80	5.98E-06	1.46E-05	4.47E-05	4.64E-19	9.30E-06	4.77E-05
100	1.18E-05	2.87E-05	7.08E-05	3.16E-18	1.79E-05	7.40E-05
120	2.06E-05	4.97E-05	1.03E-04	1.53E-17	3.06E-05	1.06E-04
140	3.28E-05	7.88E-05	1.40E-04	5.78E-17	4.80E-05	1.43E-04
160	4.90E-05	1.17E-04	1.83E-04	1.84E-16	7.07E-05	1.86E-04
180	6.98E-05	1.66E-04	2.32E-04	5.09E-16	9.94E-05	2.34E-04
200	9.58E-05	2.27E-04	2.87E-04	1.27E-15	1.35E-04	2.86E-04

Table 3b: CC probabilities – 3rd example (modified BKR)

	Modified BKR		
N	$P_{cc,1}$	$P_{cc,2}$	$P_{cc,3}$
20	0.00E+00	1.09E-07	2.19E-06
40	4.74E-23	1.02E-06	1.04E-05
60	5.96E-21	3.60E-06	2.44E-05
80	1.23E-19	8.64E-06	4.43E-05
100	1.14E-18	1.69E-05	6.98E-05
120	6.69E-18	2.92E-05	1.01E-04
140	2.90E-17	4.61E-05	1.37E-04
160	1.01E-16	6.83E-05	1.79E-04
180	3.02E-16	9.64E-05	2.26E-04
200	7.97E-16	1.31E-04	2.79E-04

VI. CONCLUSION

In this paper we study two multirate loss models for the call-level QoS assessment of the X2 link supporting Poisson arriving calls of different service-classes with fixed bandwidth requirements. Handover calls are accepted in the X2 link whenever there exists available bandwidth. Otherwise, call blocking occurs. For the evaluation of both models we compare the QoS index of congestion probabilities, under the same offered traffic-load conditions. Analytical congestion probabilities results show that both models perform equally well in most cases. As a future work we intend to apply the bandwidth reservation policy in the X2 link whereby we can achieve equalization of congestion probabilities among calls of different service-classes.

REFERENCES

1. H. Holma and A. Toskala, LTE for UMTS: Evolution to LTE – Advanced, Wiley & Sons, 2011.
2. A. Blogowski, O. Klopfenstein and B. Renard, “Dimensioning X_2 backhaul link in LTE networks”, Proc. IEEE ICC, Ottawa, Canada, June 2012.
3. M. Peng, D. Liang, Y. Wei, J. Li, and H. Chen, “Self-configuration and self-optimization in LTE-advanced heterogeneous networks”, IEEE Commun. Mag., 51 (5), pp. 36-45, May 2013.
4. I. Widjaja and H. Roche, “Sizing X2 bandwidth for Inter-connected eNBs”, Proc. IEEE VTC Fall, Anchorage, Alaska, USA, Sept. 2009.
5. B. Renard, S. Elayoubi and A. Simonian, “A dimensioning method for the LTE X2 interface”, Proc. IEEE WCNC, Shanghai, China, April 2012.
6. H. Akimaru and K. Kawashima, Teletraffic - Theory and Applications, 2nd edition, Springer, Berlin, 1999.
7. V. Frost and B. Melamed, “Traffic modeling for telecommunications networks”, IEEE Commun. Magazine, 32 (3), pp. 70-81, March 1994.
8. D. Lam, D. Cox and J. Widom, “Teletraffic modeling for personal communications services”, IEEE Commun. Magazine, 35 (2), pp. 79-87, Feb. 1997.
9. J. Kaufman, “Blocking in a shared resource environment”, IEEE Trans. Commun. 29 (10), pp. 1474-1481, Oct. 1981.
10. J. Roberts, “A service system with heterogeneous user requirements”, in: G. Pujolle (Ed.), Performance of Data Communications systems and their applications, North Holland, Amsterdam, pp.423-431, 1981.
11. M. Stasiak, M. Glabowski, A.Wisniewski, and P. Zwierzykowski, Modeling and Dimensioning of Mobile Networks, Wiley & Sons, 2011.
12. I. Moscholios, J. Vardakas, M. Logothetis and A. Boucouvalas, “A Batched Poisson Multirate Loss Model Supporting Elastic Traffic under the Bandwidth Reservation Policy”, Proc. IEEE ICC, Kyoto, Japan, 5-9 June 2011.
13. I. Moscholios, J. Vardakas, M. Logothetis and M. Koukias, “A Quasi-random Multirate Loss Model supporting Elastic and Adaptive Traffic under the Bandwidth Reservation Policy”, Int. Journal on Advances in Networks and Services, vol. 6, no. 3 & 4, pp. 163-174, December 2013.
14. D. Tsang and K. Ross, “Algorithms to determine exact blocking probabilities for multirate tree networks”, IEEE Trans. Commun., 38 (8), pp. 1266-1271, Aug. 1990.
15. J. Ni, D. Tsang, S. Tatikonda and B. Bensaou, “Optimal and structured call admission control policies for resource-sharing systems”, IEEE Trans. on Commun., 55 (1), pp. 158-170, Jan. 2007.
16. I. Moscholios, M. Logothetis, J. Vardakas and A. Boucouvalas, “Performance metrics of a multirate resource sharing teletraffic model with finite sources under the threshold and bandwidth reservation policies”, IET Networks, 4 (3), pp. 195-208, May 2015.
17. J. Kaufman and K. Rege, “Blocking in a shared resource environment with batched Poisson arrival processes”, Performance Evaluation, 24 (4), pp. 249-263, February 1996.
18. I. Moscholios, G. Kallos, V. Vassilakis and M. Logothetis, “Congestion Probabilities in CDMA-based networks supporting batched Poisson input traffic”, Wireless Personal Communications, 79 (2), pp. 1163-1186, Nov. 2014.
19. M. Mehmet-Ali. "Call–burst blocking and call admission control in a broadband network with bursty sources", Performance Evaluation, 38 (1), pp. 1-19, September 1999.
20. I. Moscholios, P. Nikolaropoulos and M. Logothetis, “Call level blocking of ON-OFF traffic sources with retrials under the complete sharing policy”, Proc. 18th ITC, Berlin, Germany, 31 August – 5 September 2003.
21. X. Li, U. Toseef, D. Dulas, W. Bigos, C. Gorg, A. Timm-Giel and A. Klug, “Dimensioning of the LTE access network”, Telecommunication Systems, 52 (4), pp. 2637-2654, April 2013.
22. M. Zonoozi and P. Dassanayake, “User mobility modeling and characterization of mobility patterns”, IEEE Journal on Selected Areas in Communications, 15 (7), pp. 1239-1252, Sept. 1997.
23. K. Yeung and S. Nanda, “Channel management in microcell/macrocell cellular radio systems”, IEEE Trans. Veh. Tech., 45 (4), pp. 601-612, Nov. 1996.
24. R. Thomas, H. Gilbert and G. Mazziotto, “Influence the movement of the mobile station on the performance of a radio cellular network”, Proc. 3rd Nordic Seminar, paper 9.4, Copenhagen, Denmark, Sept. 1988.
25. H. Xie and D. Goodman, “Mobility models and biased sampling problem”, Proc. 2nd Int. Conf. on Universal Personal Commun., Ottawa, Canada, Oct. 1993.
26. R. Roy, Handbook of Mobile Ad Hoc Networks for Mobility Models, Springer, 2011.